



Contents lists available at ScienceDirect

Journal of Quantitative Spectroscopy & Radiative Transfer

journal homepage: www.elsevier.com/locate/jqsrt

Frequency and size distribution dependence of visible and infrared extinction for astronomical silicate and graphite grains

Ashim K. Roy^a, Subodh K. Sharma^{b,*}, Ranjan Gupta^c^a Indian Statistical Institute, 203, BT Road, Kolkata 700108, India^b S N Bose National Centre for Basic Sciences, Kolkata 700098, India^c Inter University Centre for Astronomy and Astrophysics, Pune 411007, India

ARTICLE INFO

Article history:

Received 15 September 2009

Received in revised form

7 November 2009

Accepted 11 November 2009

Keywords:

Interstellar grains

Extinction spectrum

Size distribution dependence

ABSTRACT

In a recent paper, the frequency and size distribution dependence of extinction spectra for astronomical silicate and graphite grains was analyzed in the context of MRN type interstellar dust models in the far ultraviolet and ultraviolet regions. These grains were taken to be homogeneous spheres following a power law size distribution. In the present work we extend the analysis further to cover the visible as well as the infrared part of the electromagnetic spectrum. The analytic formulas presented here along with those given in the earlier paper would enable one to evaluate extinction for these grains within a wider wavelength range 1000–22,500 Å and analyze the observational interstellar extinction data in far greater details.

© 2009 Elsevier Ltd. All rights reserved.

1. Introduction

The frequency and size distribution dependence of the extinction for astronomical silicate and graphite grains was presented by us in [1] (hereafter referred as RSG-1) by way of some analytic formulas covering the far ultraviolet and the ultraviolet region (1000–4000 Å). The analysis and hence the formulas are applicable in two component interstellar dust models like Mathis, Rumble and Nordsieck (MRN) [2] models, wherein one assumes bare silicate and graphite particles to be homogeneous spheres, obeying a power law distribution with exponent -3.5 , having a minimum (a_0) and maximum (a_m) of radius. In our analysis, the admitted ranges of a_0 and a_m are quite appropriate to MRN type models. A comparison *vis-a-vis* exact Mie computations showed that the predictions of all the formulas are quite accurate. Hence, these formulas can be efficiently used for assessment of the extinction contributions of the silicate and graphite

components in investigation and building of MRN type models. It may be mentioned here that analytic formulas fitting the extinction spectra of several stars have been obtained in the past by Cardelli et al. [3] and Fitzpatrick and Massa [4], but it is recognized that these parametrizations are mathematical schemes only and do not provide added physical insight into the problem.

In the present paper, we have extended the RSG-1 analysis further to cover the visible (4000–8000 Å) as well as infrared (8000–22,500 Å) wavelengths. This will enable one to make more precise and elaborate model investigations and model building. It may be mentioned here that although the original MRN paper restricted itself to the wavelength range 1100–10,000 Å, subsequently MRN type models have been found to be useful over the entire wavelength range 1000–22,500 Å. This paper has been organized as follows. Section 2 describes the dust model contextually. Section 3 contains all the relevant functional forms of extinction obtained in terms of the size distribution parameters as well as the frequency for both graphite and silicate grains. Subsequently, numerical results of extinction obtained from these formulas are compared with exact Mie theory computations and the possible use of such formulas for individual components

* Corresponding author.

E-mail addresses: ashim@isical.ac.in (A.K. Roy), sharma@bose.res.in (S.K. Sharma), rag@iucaa.ernet.in (R. Gupta).

to multi-component system has been demonstrated in Section 4 by reviewing the average interstellar extinction spectra observational data within our analytic framework. Finally, we conclude by summarizing and discussing the results of this paper in Section 5.

2. The dust model

A classic model of interstellar dust was proposed more than 30 years ago by Mathis, Rumpl and Nordsieck (MRN) [2]. Since then, the basic model is being used even today albeit with some modifications. It has not been fully superseded by later studies. The MRN model essentially uses two separate populations of bare silicate and graphite spherical grains with a power-law distribution of their sizes having the form:

$$f(a) \propto a^{-3.5}, \quad a_0 \leq a \leq a_m, \quad (1)$$

where a is the radius of the spherical grain varying within the limits a_0 (minimum radius) and a_m (maximum radius). The admitted size ranges are

$$\text{Graphite grains : } a_0 \sim 0.005 \mu\text{m}, \quad a_m \sim 0.25 \mu\text{m}, \quad (2)$$

$$\text{Silicate grains : } a_0 \sim 0.005 \mu\text{m}, \quad a_m \sim 0.25 \mu\text{m}. \quad (3)$$

Further, the graphite material is taken to be present in two distinct structural varieties within the specified range of a_0 and a_m . This plausibility lies in the fact that graphite is a highly anisotropic material. The refractive index of graphite, therefore, depends on the orientation of electric field relative to the structural symmetry. Owing to difficulties in calculations of exact scattering quantities due to anisotropy, researchers have taken resort to an approximation known as “ $\frac{1}{3}-\frac{2}{3}$ ” approximation [5]. In this approximation, graphite grains are represented as a mixture of isotropic spheres, of which $\frac{1}{3}$ have refractive index $m = m_{\parallel}$ (referred to as graphite parallel) and $\frac{2}{3}$ have the refractive index $m = m_{\perp}$ (referred to as graphite perpendicular). This modification effectively makes MRN model a three component model. The validity of “ $\frac{1}{3}-\frac{2}{3}$ ” approximation is based on the work of Draine and Malhotra [5] who examined its accuracy in the frequency range $3.3-5.9 \mu\text{m}^{-1}$ and found the errors to be less than 6%. Outside this frequency range no investigation seems to have been done. However, in examining the dust extinction spectrum, the approximation is to be applied over the entire frequency range.

3. Extinction as a function of frequency and size distribution parameters

Exact extinction coefficient, K_{ext} , was obtained using the formula,

$$K_{\text{ext}}(\lambda) = \pi N \int_{a_0}^{a_m} Q_{\text{ext}}(x) a^2 f(a) da, \quad (4)$$

where $Q_{\text{ext}}(x)$ is the extinction efficiency of an individual scatterer of size parameter $x = 2\pi a/\lambda$ with λ as the wavelength of the radiation. The exact extinction efficiency Q_{ext} for a spherical homogeneous scatterer can be computed using Mie formulas. The necessary refractive

index particulars for the various components (at various wavelengths) were taken from the tables provided by Draine [6] on his website. The number of particles per unit volume, N has been arbitrarily fixed at $N = 4.4 \times 10^8$. Clearly, N being just a multiplicative constant, its admitted value does not make any effective difference in the functional form of K_{ext} we wish to determine.

As in RSG-I, here also our approach has been to study the $K_{\text{ext}}-v$ graph for each material component separately within allowable ranges of a , which means properly varying a_0 and a_m . It can be easily verified that for the power-law size distribution, $f(a) = ca^{-3.5}$, the moments of the distribution are simple algebraic functions of a_0 and a_m/a_0 [1]. Consequently, with a functional form $K_{\text{ext}}(a_0, a_m, v)$, our investigations reveal that the extinction in the visible and infrared regions for the materials considered have the following general form:

$$K_{\text{ext}} = C N a_0^{5/2} [\phi(a_0, v) + \psi(a_m, v)]. \quad (5)$$

The functions ϕ and ψ have forms which change in various frequency sub-intervals. For each component of graphite (parallel and perpendicular), three formulas were needed to fit extinction. For silicate, two formulas were sufficient. Several values of a_m and a_0 were considered. Formulas presented here are valid in the size limits:

$$\text{Graphite grains : } 0.002 \mu\text{m} \leq a_0 \leq 0.005 \mu\text{m}, \\ 0.15 \mu\text{m} \leq a_m \leq 0.25 \mu\text{m}, \quad (6)$$

$$\text{Silicate grains : } 0.004 \mu\text{m} \leq a_0 \leq 0.006 \mu\text{m}, \\ 0.2 \mu\text{m} \leq a_m \leq 0.4 \mu\text{m}. \quad (7)$$

Observations of the spectra suggested that the functions $\phi(a_0, v)$ and $\Psi(a_m, v)$ can have the simple forms:

$$\phi(a_0, v) = b_0(v) + a_0^{1/2} b_1(v) + a_0 b_2(v),$$

$$\Psi(a_m, v) = \frac{c_0(v)}{a_m^{1/2}} + \frac{c_1(v)}{a_m} + \frac{c_2(v)}{a_m^2} + \frac{c_3(v)}{a_m^3} + \dots,$$

where a_0, a_m are taken in units of 10^{-5} cm, v in units of 10^5 cm^{-1} . The number of significant terms in ϕ and Ψ contributing to the extinction depend on the material as well as the frequency interval considered. The forms of $\phi(a_0, v)$ and $\Psi(a_m, v)$ have been constructed by careful analysis of the regional (frequency subintervals) behavior of the extinction for each of the materials considered. In the process of developing analytic formulas, care has also been taken to have a good compromise between accuracy and calculational simplicity so that our analysis could be applied expediently for purposeful dust modeling within the power law framework considered here.

Following relationships have been obtained:

3.1. Homogeneous graphite grains with refractive index $m = m_{\perp}$

1. For $4000 \leq \lambda \leq 8000 \text{ \AA}$ (visible):

$$K = C a_0^{5/2} [-0.02738 v a_0^{1/2} (1 + 2.5647 a_0^{1/2}) (1 + 3.4328 v^{1/2}) \\ + v (0.37707 - 0.02357 a_m^{1/2} + 0.045 a_m) \\ + a_m (0.002808 - 0.12 v^2) - 0.02845 / a_m^{3/2}]. \quad (8)$$

2. For $8000 \leq \lambda \leq 12,500 \text{ \AA}$ (infrared I):

$$K = Ca_0^{5/2}[-0.16941v^{3/2}(2.6493a_0 + a_0^{1/2}) + 4.2(v-0.08)(0.125-v)(a_m-1.5)(2.77-a_m) + v(0.33934 + 0.14006a_m - 0.035086a_m^2) + 0.05636/a_m^{1/2} - 0.237187/a_m^{3/2} + 0.17054/a_m^{5/2}]. \quad (9)$$

3. For $12,500 \leq \lambda \leq 22,500 \text{ \AA}$ (infrared II):

$$K = Ca_0^{5/2}[-a_0^{1/2}v^{3/2}(0.4083a_0^{1/2} + 0.1798) + v(1.12315 - 1.104/a_m - 0.043a_m) + 5(v-0.044)(0.08-v)(a_m-2.45)(a_m-1.0) - 0.12273/a_m + 0.133/a_m^{3/2}]. \quad (10)$$

3.2. Homogeneous graphite grains with refractive index $m = m_{||}$

1. For $4000 \leq \lambda \leq 8000 \text{ \AA}$ (visible):

$$K = Ca_0^{5/2}[-1.10a_0^{1/2}v^3 + 3.6927(v^{1/2} - 0.3535)(0.5 - v^{1/2}) \times (a_m - 1.4535/a_m)(1/a_m^{1/2} - 0.6329) + v(0.8978/a_m^{1/2} - 0.617/a_m + 0.1737/a_m^{3/2}) - 0.07946/a_m^{1/2} + 0.02357a_m^{1/2} - 0.00939/a_m^{3/2}]. \quad (11)$$

2. For $8000 \leq \lambda \leq 12,500 \text{ \AA}$ (infrared I):

$$K = Ca_0^{5/2}[v(1.5635/a_m^{1/2} - 1.9781/a_m^{3/2}) - 0.18925/a_m + 0.00713 + 0.236022/a_m^2 + 8.0(v-0.08)(v-0.125)(a_m-1.0)(2.5-a_m)]. \quad (12)$$

3. For $12,500 \leq \lambda \leq 22,500 \text{ \AA}$ (infrared II):

$$K = Ca_0^{5/2}[v^2[-0.1a_0^{1/2} + v^3a_m(32.95 + 49.571a_m^3) + a_m(0.099423 - 0.004578a_m^2 + 0.002301a_m^3)]. \quad (13)$$

3.3. Homogeneous silicate grains

1. For $4000 \leq \lambda \leq 8000 \text{ \AA}$ (visible):

$$K = Ca_0^{5/2}[a_m(0.02884 - 0.02613a_m + a_m^2) - va_m^{3/2}(0.2673 - 0.2268a_m + 0.0365a_m^2) + v^2a_m^2(2.73017 - 3.06825a_m^{1/2} + 0.8417a_m)]. \quad (14)$$

2. For $8000 \leq \lambda \leq 22,500 \text{ \AA}$ (infrared):

$$K = Ca_0^{5/2}[0.0004 - 0.0016v^{1/2} - 0.007871a_0^{1/2}v + 0.01835a_m^{1/2}v - a_m^{3/2}v^2(0.2323 - 1.8104va_m + 2.0856v^2a_m^2)]. \quad (15)$$

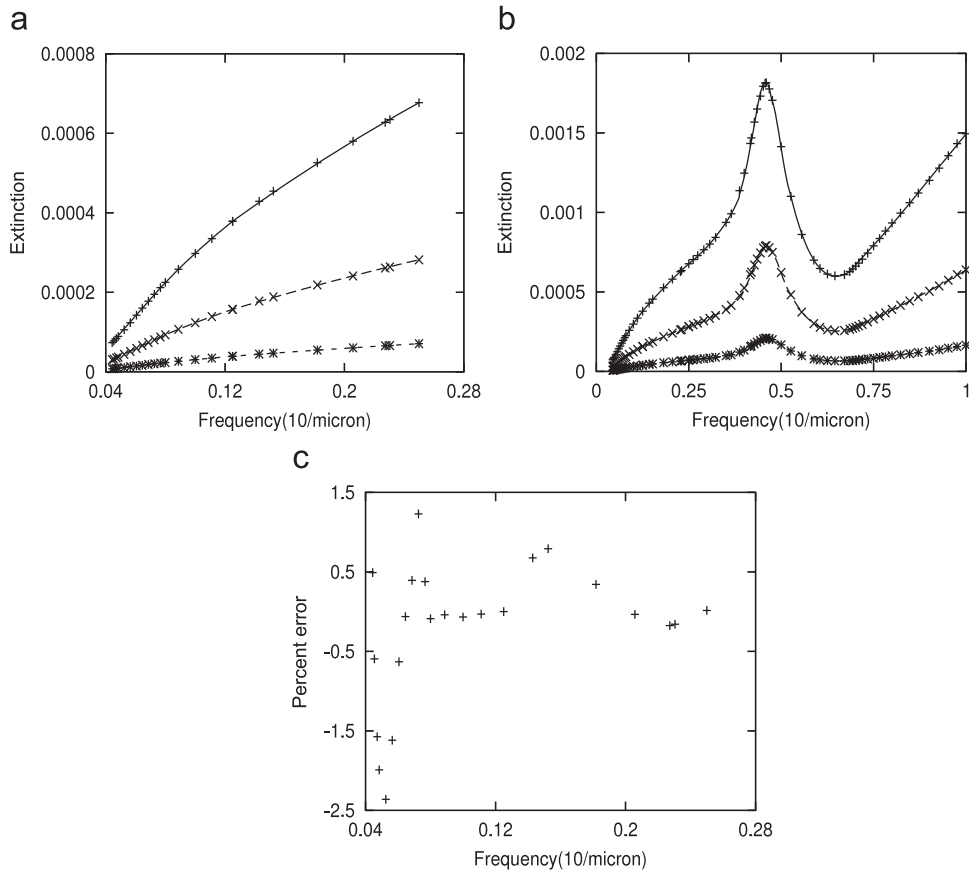


Fig. 1. (a) Comparison of predictions of Eqs. (8)–(10) with exact computations from (4) in the IR and visible regions of spectra. Solid lines are predictions and points are exact computations. In this figure, $a_m = 0.25 \mu\text{m}$ and $a_0 = 0.005 \mu\text{m}$ (solid line), $a_0 = 0.0035 \mu\text{m}$ (large dashed line) and $a_0 = 0.002 \mu\text{m}$ (small dashed line). (b) Same as (a) but for entire extinction spectrum covering IR, V, UV and FUV regions. (c) Percent errors in Eqs. (8)–(10) with respect to exact computations from (4). In this figure, $a_m = 0.25 \mu\text{m}$ and $a_0 = 0.005 \mu\text{m}$.

In all the above formulas (8)–(15), $C = \pi N/10^8$; a_0 , a_m are in units of 10^{-5} cm; ν in units of 10^5 cm $^{-1}$.

4. Numerical comparisons

We divide this section into two parts. The first part viz. Section 4.1 contains the formal details in respect of examining the results of the analytic formulas presented in this paper and contrasting them with the corresponding exact Mie results. The second part viz. Section 4.2 contains illustration of the average interstellar extinction spectra analyzed through the two component MRN (silicate-graphite) model by direct use of the analytic formulas for extinction developed by us in this paper as well as in RSG-I.

4.1. Verification of the formulas

Fig. 1a shows a comparison of exact extinction curves with predictions of formulas (8)–(10) for graphite perpendicular grains. The three graphs presented in this figure are for $a_0 = 0.002$, 0.0035 and 0.005 μm with fixed value of $a_m = 0.25$ μm . It can be seen that the agreement between exact results and predictions of formulas is

excellent. Although not shown here, it has been noted that while the variation in a_0 results in bigger changes in extinction, the variation in extinction due to changes in a_m is comparatively much weaker. In Fig. 1b we have combined our earlier results [1] with the present ones to have the full spectrum over 1000–22,500 Å. Fig. 1c shows percent error in respect of Fig. 1a with $a_0 = 0.005$ μm and $a_m = 0.25$ μm . In the same order Figs. 2a–c are for graphite parallel and Figs. 3a–c are for the silicate. In Figs. 3a and b, the three admitted values of a_0 are 0.004 , 0.005 and 0.006 μm with fixed $a_m = 0.30$ μm . Fig. 3c shows percent error in respect of Fig. 3a with $a_0 = 0.005$ μm and $a_m = 0.30$ μm . For Figs. 2a and 3a, computations have been performed using formulas (11)–(13) and (14)–(15). The percent error, depicted in the Figs. 1c, 2c and 3c, has been defined as

$$\text{Percent error} = \frac{[K_{\text{ext}}(\text{exact}) - K_{\text{ext}}(\text{formula})] \times 100}{K_{\text{ext}}(\text{exact})}$$

Predictions of formula can be seen to be extremely good. In general, the error is within 1% but for a few regions it can go up to about 3%. The results shown are representative results only. However, it has been verified that this result is valid for entire range of a_0 and a_m values considered in this work.

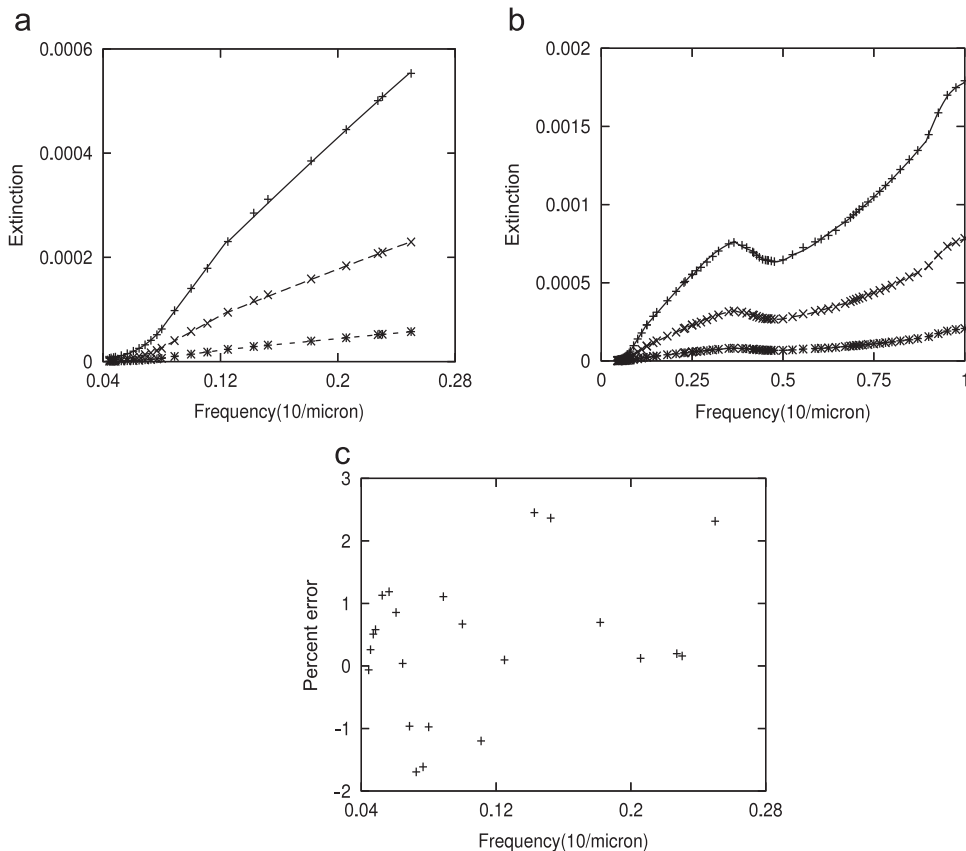


Fig. 2. (a) Comparison of predictions of Eqs. (11)–(13) with exact computations from (4) in the IR and visible regions of spectra. Solid lines are predictions and points are exact computations. In this figure, $a_m = 0.25$ μm and $a_0 = 0.005$ μm (solid line), $a_0 = 0.0035$ μm (large dashed line) and $a_0 = 0.002$ μm (small dashed line). (b) Same as (a) but for entire extinction spectrum covering IR, V, UV and FUV regions. (c) Percent errors in Eqs. (11)–(13) with respect to exact computations from (4). In this figure, $a_m = 0.25$ μm and $a_0 = 0.005$ μm .

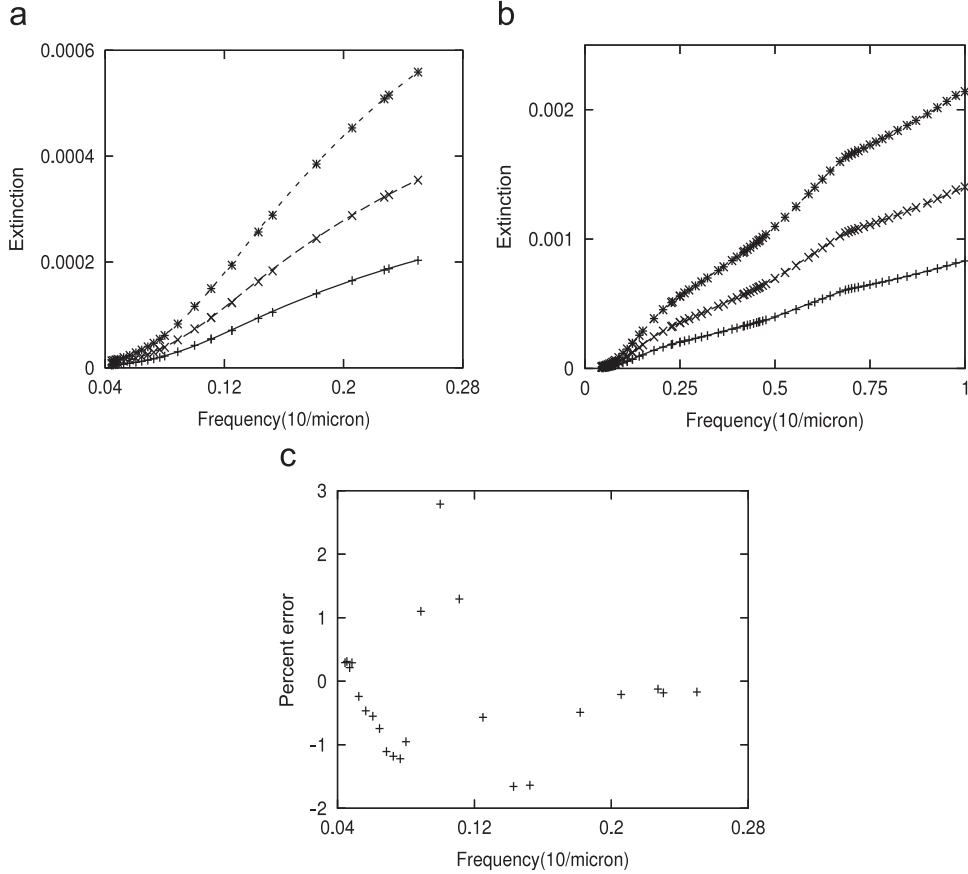


Fig. 3. (a) Comparison of predictions of Eqs. (14) and (15) with exact computations from (4). Solid lines are predictions and points are exact computations. In this figure, $a_m = 0.30 \mu\text{m}$ and $a_0 = 0.006 \mu\text{m}$ (solid line), $a_0 = 0.005 \mu\text{m}$ (large dashed line) and $a_0 = 0.004 \mu\text{m}$ (small dashed line). (b) Same as in (a) but for entire extinction spectrum. That is covering IR, V, UV and FUV regions. (c) Percent errors in Eqs. (14) and (15) with respect to exact computations from (4). In this figure, $a_m = 0.3 \mu\text{m}$ and $a_0 = 0.005 \mu\text{m}$.

4.2. Applications to the observational data on the average interstellar extinction spectrum

The average interstellar extinction spectrum data in [7] has $A(\lambda)/A(V)$ (absolute extinction) details which may be investigated by direct use of the various extinction formulas developed by us. Here $A(\lambda)$ is proportional to $K_{\text{ext}}(\lambda)$ and $A(V)$ is the extinction at $0.55 \mu\text{m}$ wavelength. The normalized extinction is defined as $E(\lambda-V)/E(B-V)$ where $E(\lambda_1-\lambda_2) = A(\lambda_1) - A(\lambda_2)$.

In the two component MRN silicate-graphite model framework the input data adopted as the relative abundance constant is [8]

$$\frac{\text{Graphite mass}}{\text{Silicate mass}} = 0.53$$

and for both silicate and graphite grains the size distribution parameters are

$$a_0 = 0.05 \times 10^{-5} \text{ cm}, \quad a_m = 2.5 \times 10^{-5} \text{ cm}.$$

If N_g and N_s are the particle numbers for graphite and silicate, respectively, then, the relative mass abundance ratio can be cast into the relative number ratio

$N_s/N_g = 1.2922$ (densities are taken as 2.26 for graphite and 3.30 for silicate).

In our extinction formulas, we use the model specified values of a_0 and a_m . Thereafter, selecting $\nu (= 1/\lambda)$, total extinction from the graphite grains can be written as

$$K_{\text{ext}}^g(\lambda) = N_g \left[\frac{2}{3} K_{\text{ext}}^{g_1}(\lambda) + \frac{1}{3} K_{\text{ext}}^{g_2}(\lambda) \right]$$

and the total extinction from the silicate grains can be written as

$$K_{\text{ext}}^s(\lambda) = N_s K_{\text{ext}}^s(\lambda),$$

where $K_{\text{ext}}^{g_1}$, $K_{\text{ext}}^{g_2}$, K_{ext}^s are all evaluated using the appropriate formulas. Hence the absolute extinction produced by the silicate-graphite particles of the model for the wavelength λ is

$$K_{\text{ext}}(\lambda) = N_g [K_{\text{ext}}^g(\lambda) + 1.2922 K_{\text{ext}}^s(\lambda)].$$

The $K_{\text{ext}}(\lambda)$ so obtained can be used to compute $K_{\text{ext}}(\lambda_1)/K_{\text{ext}}(\lambda_2) (\equiv A(\lambda_1)/A(\lambda_2))$ for any selected pair of wavelengths (λ_1, λ_2) and can be compared with the corresponding observed data given in [7]. Notice that the value of N_g or N_s is not directly needed in computation of the ratio. We have selected three wavelengths

$(\lambda_1, \lambda_2, \lambda_3)$ in each of the four regions (viz. FUV, UV, V, IR) so as to have a coverage of the corresponding region. Thus, in each region, the two ratios $A(\lambda_1)/A(\lambda_2), A(\lambda_2)/A(\lambda_3)$ are compared with the corresponding observed data. This is a sort of region-wise consistency check for the parameter values of a_0, a_m used in this model. The comparative data for $A(\lambda_1)/A(\lambda_2)$ are shown in Table 1. It may be observed that for a two component model the agreement is reasonably good between numbers obtained from the observational data and that obtained by the use of our formulas. A regional inconsistency, if present, would indicate that a gross correction is needed in respect of selection of the input parameters.

Finally, we have used the appropriate ratio $A(\lambda)/A(V=0.55\ \mu\text{m})$ to compare the observational spec-

trum data and predictions from our formulas for the value $R_V=3.05$. The quantity compared is the normalized extinction $E(\lambda-B)/E(B-V)$. The wavelength corresponding to B is $0.44\ \mu\text{m}$. The results of this comparison are depicted in Fig. 4. The agreement between data points and the predicted curve from formulas is reasonably good. We have noted that the slight discrepancy seen in the FUV region can be minimized by a little readjustment of a_0 around the value admitted in the model. However, we did not try with any systematic fitting reckoning that it would not be a meaningful exercise unless and until PAHs are included in the model.

5. Conclusions and discussions

In this work, we have presented the extinction spectrum analysis for astronomical silicate and graphite grains in the wavelength range $4000\text{--}22,500\ \text{\AA}$ which covers the visible and the infrared regions of the extinction spectra of these grains. The grain size distribution range covered by us is in keeping with the acceptable compositional aspects of interstellar dust models corresponding to the average interstellar extinction spectra data. From this point of view, we feel that the results and the analytic formulas presented in this paper, together with RSG-I, would have application-worthiness in the sense that accurate estimates of extinction contributions for these material components in the extinction spectrum for interstellar dust can be made directly in terms of the frequency and the size distribution parameters. Needless to say, a complete account of the extinction contributions made by each material component in respect of the various dust models (which are considered to be possible candidates) are needed for ascertaining their effectiveness in reproducing the corresponding interstellar dust extinction spectra data reliably. This necessitates some more investigative work-outs and mathematical analyzes (may be similar in nature as provided by us in this work) to be

Table 1
A comparison of $A(\lambda_1)/A(\lambda_2)$ from data in [6] with that obtained from formulas.

λ (μm)	$(\lambda_1, \lambda_2\ \mu\text{m})$	$A(\lambda_1)/A(\lambda_2)$ (data)	$A(\lambda_1)/A(\lambda_2)$ (formula)
FUV			
0.111	(0.111,0.149)	1.4173	1.474
0.149	(0.149,0.190)	1.0192	1.044
0.190			
UV			
0.210	(0.210,0.274)	1.505	1.4172
0.274	(0.149,0.190)	1.2704	1.263
0.344			
V			
0.440	(0.440,0.550)	1.330	1.2982
0.550	(0.550,0.700)	1.3514	1.3798
0.700			
IR			
0.900	(0.900,1.250)	1.8462	1.793
1.250	(1.250,1.650)	1.7333	1.7333
1.650			

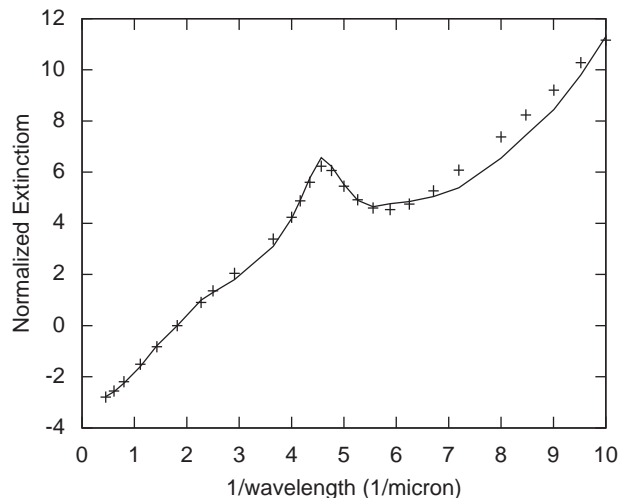


Fig. 4. A comparison of the observed average interstellar extinction data and that obtained using our formulas. The data are from [7] and the model parameters are from [8].

carried out with the remaining important dust constituents also. Our analysis of the observed average interstellar extinction spectrum indicates that there are indeed some small discrepancies with the simple two component MRN model. In this respect, we motivate ourselves to study the PAHs extinction so that the MRN models extended by PAHs could also be analyzed using direct analytic extinction formulas.

We feel that this analysis could also be extended to more complex distributions advocated by some researchers [9,10]. In the present work, we have restricted ourselves to the power-law distribution for substantive demonstration of workability of the formulas developed by us. It is our wish to extend this analysis further to cover some more variants of the power-law distribution like the log-normal, the truncated (upper as well as lower) power-law and ascertain their effectiveness in a comparative context *vis-a-vis* the simple power-law distribution.

References

- [1] Roy AK, Sharma SK, Gupta R. A study of frequency and size distribution dependence of extinction for astronomical silicate and graphite grains. *J Quant Spectrosc Radiat Transf* 2009;110:1733–40.
- [2] Mathis JS, Rumpl W, Nordsieck KH. The size distribution of interstellar grains. *ApJ* 1977;217:425–33.
- [3] Cardelli JA, Clayton GC, Mathis JS. The relationship between infrared, optical and ultraviolet extinction. *ApJ* 1989;345:245–56.
- [4] Fitzpatrick EL, Massa D. An analysis of the shapes of interstellar extinction curves. V. The IR-through-UV curve morphology. *ApJ* 2007;663:320–41.
- [5] Draine BT, Malhotra S. On graphite and the 2175 Å extinction profile. *ApJ* 1993;414:632–45.
- [6] Draine BT at <<http://www.astro.princeton.edu/draine>>.
- [7] Whittet DCB. *Dust in galactic environments*, 1st ed. IOP; 2002.
- [8] Di Bartolomeo A, Barbaro G, Perinotto M. Internal extinction in spiral dust galaxies. *MNRAS* 1995;277:1279.
- [9] Mathis JS. Dust models with tight abundance constraints. *ApJ* 1996;472:643–55.
- [10] Weingartner JC, Draine BT. Dust grain-size distributions and extinction in the milky way, large magellanic cloud and small magellanic cloud. *ApJ* 2001;548:296–309.